ACS APPLIED ENERGY MATERIALS

www.acsaem.org Article

Analytical Evaluation of Lead Iodide Precursor Impurities Affecting Halide Perovskite Device Performance

Ross A. Kerner, Earl D. Christensen, Steven P. Harvey, Jonah Messinger, Severin N. Habisreutinger, Fei Zhang, Giles E. Eperon, Laura T. Schelhas, Kai Zhu, Joseph J. Berry, and David T. Moore*

Cite This: *ACS Appl. Energy Mater.* 2023, 6, 295−301 Read Online

ACCESS | Metrics & More | Article Recommendations | Supporting Information

ABSTRACT: Mirroring established semiconductor technologies, using higher quality reagents to synthesize halide perovskite materials results in improved optoelectronic performance. In this study, we selected five different commercial PbI_2 sources of various purities and fabricated solar cells in three different perovskite composition-device architecture combinations. In all cases, we observed similar device performance correlations to the PbI_2 reagent source across the different processing recipes and architectures. We then employed a suite of analytical characterization techniques to determine the identity and concentration of impurities within the PbI_2 reagents that affected the device performance trends. Many impurities were observed; some remain unidentified, but it was possible to single out acetate (OAc) and potassium (K) as key species displaying the largest variation in concentrations among the as-received PbI_2. Acetate was identified as a detrimental impurity, while K impurities may be advantageous as suggested by the previous literature on alkali cation additives. A simple aqueous recrystallization successfully decreased the concentration of many impurities, and the results from devices fabricated from recrystallized PbI_2 reagents are interpreted in terms of their new impurity profiles. This work significantly contributes to the list of known impurities in perovskite reagents that researchers should be aware of, and we propose improved purification methods for perovskite precursors will further benefit device performance, run-to-run, and batch-to-batch reproducibility.

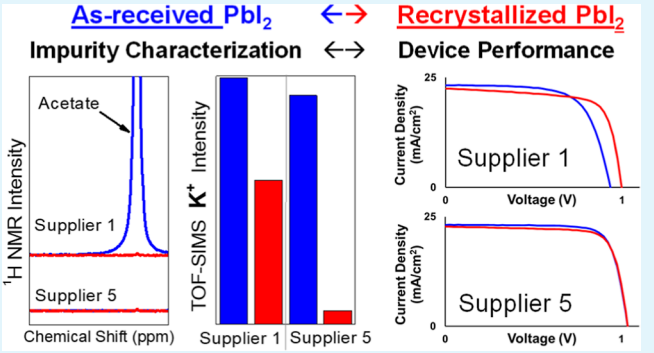

KEYWORDS: *PbI2 reagent source, lead iodide precursor impurities, halide perovskite; device performance, SIMS data*

INTRODUCTION

Halide perovskite materials are touted as tolerant to the presence of native structural defects; native refers to "intrinsic" lattice point defects, including vacancies and interstitials, which may or may not be induced by an extrinsic impurity/defect.[1−3] That is to say, with the possible exception of positively charged iodine interstitials,[4] native defects are optoelectronically inert and do not prevent these materials from performing their primary photovoltaic or electroluminescent function.[1] This limited tolerance to crystallographic imperfections may mean native defects in perovskites are superficially benign, but their interactions with extrinsic species are certainly consequential. Reactions between native halide vacancies and molecular oxygen influence doping[5] and facilitate degradation.[6,7] Moreover, it is understood that concentrations of native defects and extrinsic impurities are directly linked. Ionic conductivity measurements of undoped and doped $PbBr_2$ crystals illustrate how, for example, Na^+ impurities occupying Pb^{2+} sites induce halide vacancies for charge neutrality, which are available to participate in ionic conduction.[8] We speculate that halide perovskite defect populations are similarly dominated by extrinsic species introduced by impurities within reagents, certain additives included in the ink, and byproducts released by *in situ* reactions during synthesis. Further, a growing body of literature[9−18] indicates that the full efficiency and stability potential of halide perovskite materials will, to some degree, be unlocked by improving precursor quality, motivating us to scrutinize the impurity content of PbI_2 reagents for perovskite applications.

From this study, we present results from a semiquantitative analytical characterization of five commercially available PbI_2 materials. Three main techniques were used: inductively coupled plasma optical emission spectroscopy (ICP-OES) to determine I/Pb stoichiometry; ^1H and ^{13}C nuclear magnetic resonance (NMR) spectroscopy to reveal hydrogen-containing organic impurities; and time-of-flight secondary ion mass spectrometry (TOF-SIMS) to compare relative intensities of

Received: September 13, 2022
Accepted: November 28, 2022
Published: December 20, 2022

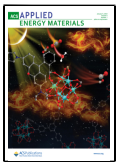

Table 1. Abbreviation (abbr.), Product Information, Stoichiometry, Solubility, and Highlighted Impurities Suggested by SIMS and NMR Data for the Five Commercial PbI_2 Sources Evaluated in This Study, Listed in Order of I/Pb Ratio Measured by ICP-OES

abbr.	supplier	purity (%)	form	I/Pb ratio[a]	solubility	confirmed impurities	suspected impurities
SA2	Sigma-Aldrich	99	powder	1.84	good	Na, K, OAc	OH^-, O^{2-}
SA5	Sigma-Aldrich	99.999	powder	1.92	poor[b]	Na, K	OH^-, O^{2-}, OAc
AA4	Alfa Aesar	99.9985	powder	1.97	poor	Na, K, organics	NO_3^-
TCI4	TCI	99.99	powder	2.03	good		organics
AA5	Alfa Aesar	99.999	beads	2.10	moderate	KI	

[a]ICP-OES data has an average error of ±5.8% with a maximum error of ±6.7%. [b]Would not dissolve in perovskite inks precluding device fabrication.

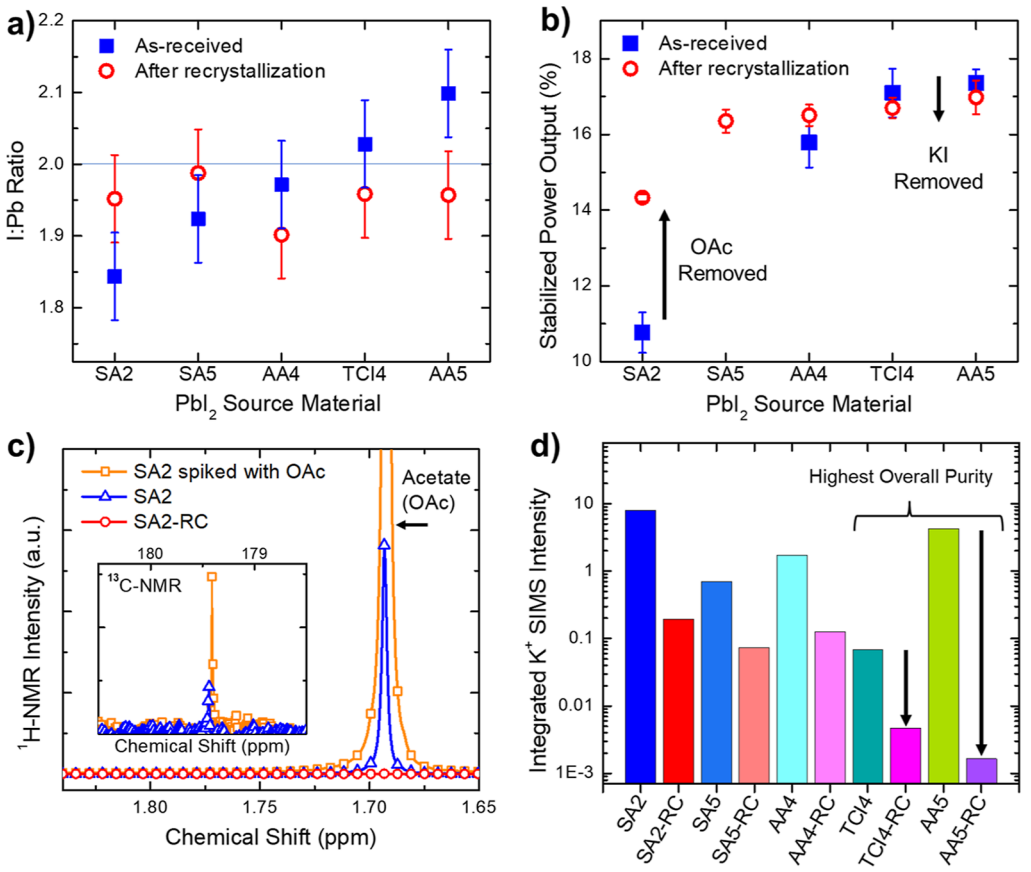

Figure 1. (a) I/Pb ratio measured by ICP-OES for as-received PbI_2 reagents compared to after aqueous recrystallization. (b) SPO averaging four champion pixels, one from each device substrate, fabricated with as-received and recrystallized PbI_2 precursors (architecture ITO/SnO_2/$Cs_{0.04}FA_{0.86}MA_{0.14}PbBr_{0.13}I_{2.82}$:Cl/spiro-MeOTAD/$MoO_x$/Al). Error bars are the standard deviation. (c) ^{1}H NMR of Sigma-Aldrich 99% PbI_2 as-received (SA2), the SA2 sample spiked with a ~3 mg particle of lead acetate trihydrate ($Pb[OAc]_2{\cdot}3H_2O$), and a sample of recrystallized SA2 (SA2-RC). (d) Integrated SIMS K^+ ion intensity (summation of K counts normalized to total ion counts over 43 data points) of the PbI_2 powders as-received and after recrystallization (denoted by -RC suffix).

lightweight atomic and molecular impurities. These techniques can be used separately or in combination to collect different pieces of information. For example, ICP-OES is ideal to quantify many elements, but molecular species, such as organics, water, hydroxide, carbonate, or nitrate, may need to be measured by other methods like NMR, ion chromatography, or titrations. A rigorous study on PbI_2 should evaluate purity along several axes for a comprehensive understanding of the impact of trace impurities on the resulting perovskite material quality and device performance.

Our analysis details two specific impurities in different source materials that were relatively abundant, positively identifiable, and successfully removed by aqueous recrystallization to measure an effect on devices. We found that iodide substoichiometry (I/Pb ratio < 2) was largely due to substitution of iodide by oxygen-containing anions, including hydroxide (OH^-), proposed previously,[11] as well as acetate (OAc) unambiguously identified in the lowest quality PbI_2 examined here. Oxidic impurities are notoriously difficult to remove from Pb halides,[19] but reducing their concentration has been shown to have a positive effect on perovskite devices.[11] In contrast, the high-quality PbI_2 sources investigated displayed relatively low concentrations of oxidic anion impurities. One PbI_2 reagent, in particular, simultaneously indicated elevated levels of potassium (K) and superstoichiometry (I/Pb > 2) suggesting KI as a plausible impurity. When oxidic anion

https://doi.org/10.1021/acsaem.2c02842
ACS Appl. Energy Mater. 2023, 6, 295−301

concentrations are low, the beneficial effect of even small amounts of alkali iodide impurities like KI[20−25] may become visible, helping to explain this PbI_2's high material quality and device performance. Simply put, the beneficial effects of K can be easily overshadowed by other impurities. This was substantiated by purifying the as-received PbI_2 sources *via* aqueous recrystallization which reduced both OAc and adventitious K, among other impurities, and amended stoichiometries nearer to 2. Finally, we compared devices fabricated from all 10 as-received and recrystallized PbI_2 sources, which, in combination with the analytical characterization, provides insights regarding dominant impurities and rationalizes expected outcomes in devices. Our work demonstrates that a competition can and does exist between beneficial (e.g., KI) and detrimental (e.g., oxidic anions) impurities, which influence the overall performance of the materials at the device level.

While we suspect some impurities remain unidentified and/or unquantified, analytical verification of key species, such as OAc and K, allowed us to better explain observed differences in precursor solubility, deviation from nominal stoichiometry, and correlations to device performance. This work additionally demonstrates that common analytical techniques provide accessible means to evaluate purity levels of perovskite precursors and that practical purification methods can effectively raise the purity of most PbI_2. These techniques are relevant to fundamental scientists for understanding the impact of synthetic conditions and intrinsic *versus* extrinsic material properties, as well as to applied scientists for tactics to improve quality control, performance, and reproducibility.

EXPERIMENTAL SECTION

See the Supporting Information for a complete description of experimental details.

RESULTS AND DISCUSSION

Abbreviations used throughout the article for the five PbI_2 products, arranged according to measured stoichiometry, are shown in Table 1, along with their nominal purity, physical form, I/Pb ratio, and impurity information inferred from our data. The nomenclature is based on the supplier name and the number of "9s" in the quoted purity using metal basis or trace metal basis when reported.

Perfectly pure stoichiometric PbI_2 should display an I/Pb ratio equal to two; therefore, stoichiometry, which we measured by ICP-OES, is an indirect measure of overall purity or quality.[15] Table 1 and Figure 1a show I/Pb ratios of the as-received PbI_2 materials varied from 8% deficient to 5% excess in iodide. Despite statistical considerations, the trend in the as-received I/Pb ratio appears to be reflected in the corresponding n−i−p solar cell device efficiency, with an architecture of tin-doped indium oxide (ITO)/tin oxide (SnO_2)/$Cs_{0.04}FA_{0.86}MA_{0.14}PbBr_{0.13}I_{2.82}$:Cl/2,2′,7,7′-tetrakis-(*N*,*N*-di-*p*-methoxyphenylamino)-9,9′-spirobifluorene (spiro-MeOTAD)/molybdenum oxide (MoO_x)/Al, in Figure 1b reported as a stabilized power output (SPO) of the champion pixels from each substrate in the device run. Note that SA5 is omitted from as-received device sets because its solubility was too low to produce films adequate for devices. The corresponding device parameters derived from current density−voltage (*J*−*V*) scans (Figure S1) show an identical trend in performance with PbI_2 source. We used the as-received PbI_2 reagents to fabricate two additional device sets with differing perovskite compositions, processing, architectures, and researchers (Figures S2 and S3 and Tables S1 and S2) confirming that the noted effects are not limited to a specific composition, architecture, nor processing details. However, this correlation to the I/Pb ratio was found to be a coincidence, as we describe below.

We subsequently performed an aqueous recrystallization of all five PbI_2 sources to remove impurities that might alter the measured stoichiometry. As shown in Figure 1a, the variation in the I/Pb ratio was successfully reduced among the newly recrystallized (RC) PbI_2 reagents. Most significant, the I/Pb ratio of the two outliers, SA2 and AA5, became statistically equivalent and much closer to the two. Devices were fabricated from the recrystallized PbI_2, and the measured SPO in Figure 1b shows the efficiency no longer correlates to the new stoichiometry (see Figure S1 for *J*−*V* parameters and statistics for the recrystallized PbI_2 devices). It is clear from the SPO and *J*−*V* parameters that recrystallization increased the performance of the SA2 reagent but slightly decreased the performance of devices made using TCI4 and AA5. In other words, the device performance was homogenized by the recrystallization process. Finally, recrystallization appears to have decreased the hysteresis relative to the as-received PbI_2 reagents, mainly due to less hysteresis in the fill factor with voltage sweep direction for AA4, TCI4, and AA5 (Figure S1).

However, though it is significantly less drastic, the recrystallized performance trend resembles that observed for the as-received reagents. Note the recrystallized device data includes SA5 that became soluble after recrystallization, and the solubility of AA4 also improved slightly, which is a consistent improvement observed by several groups.[11,13] This set of experiments illustrates that the I/Pb ratio of the PbI_2 reagent has some influence on the perovskite quality, but it is not a reliable indicator of device efficiency. Device level metrics are likely dependent on the specific impurities that alter I/Pb ratio, so we turned to more in-depth characterization techniques to reveal the identity of the dominant impurity species in each PbI_2 source.

Using ^{1}H NMR, we identified OAc as a major anionic impurity in as-received SA2 (Figure 1c), which we confirmed by spiking with lead acetate trihydrate and additional ^{13}C NMR (inset). Acetate is likely remnant from PbI_2 synthesis, which commonly involves mixing water soluble $Pb(OAc)_2$ or $Pb(NO_3)_2$ salts with KI to precipitate PbI_2.[12−14,26,27] Spiking experiments quantified the OAc concentration as ∼2.2 ± 0.3 mol % with respect to Pb (Figure S4). It is particularly interesting to note the agreement between our inferred synthetic origin of SA2 and reports by Eckstein *et al.* that the $Pb(OAc)_2$ route to PbI_2 typically results in a lower stoichiometry than *via* $Pb(NO_3)_2$.[27] The measured amount of OAc accounts for only one-fourth of the full 8% iodide deficiency in SA2, implying other extrinsic impurities are present in similar percentages (plausibly PbO or PbIOH). Figure 1c additionally shows that OAc was largely removed by the aqueous recrystallization to which we partially attribute the increase in stoichiometry and improved device performance for SA2 (Figure 1a,b). Because the OAc concentration, by itself, does not fully explain the device performance trends, either before or after recrystallization, we performed TOF-SIMS to identify species not detectable by NMR. Using TOF-SIMS has two advantages: (1) the sample does not need to be digested, which is often a source of significant K contamination, and (2)

https://doi.org/10.1021/acsaem.2c02842
ACS Appl. Energy Mater. 2023, 6, 295−301

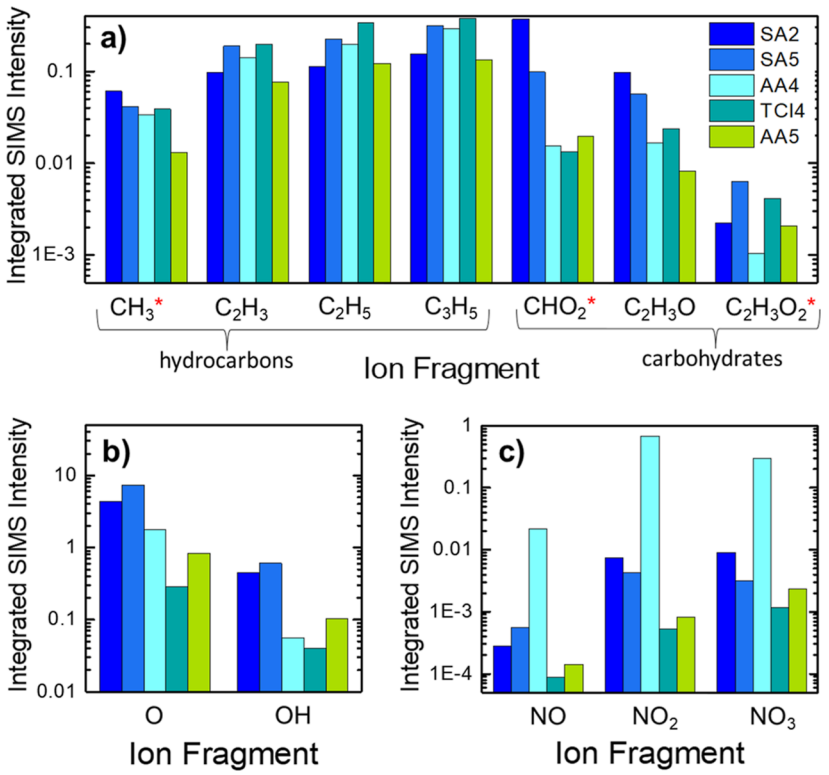

Figure 2. Integrated ion fragment SIMS intensities of (a) hydrocarbons and carbohydrates, (b) oxide and hydroxide, and (c) nitrogen oxides in the as-received PbI_2 sources. The fragments associated with acetate are indicated by * in (a).[28] Either TCI4 or AA5 displays the lowest intensity for each fragment.

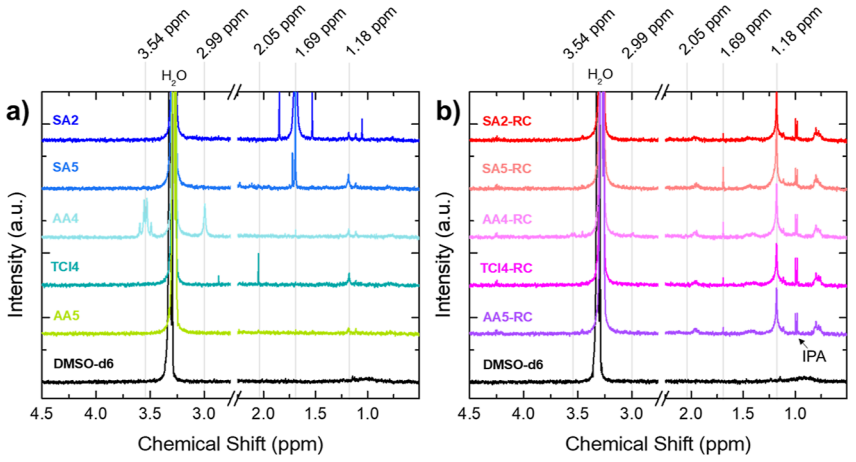

Figure 3. Upfield region ^1H NMR spectra of PbI_2 sources as-received (a) and after aqueous recrystallization (b) denoted by -RC suffix (in deuterated DMSO [DMSO-d_6]). The DMSO-d_5 solvent peak is omitted by the *x*-axis break and several impurity peak positions are indicated for clarity.

there is no interference from Ar isotopes (from the plasma in ICP) when detecting variations in K.

The most notable impurity we identified with TOF-SIMS was K, which also likely originates from synthesis, showing significantly larger variations between PbI_2 samples compared to other impurities detected with TOF-SIMS. Figure 1d shows the integrated K^+ intensity of the PbI_2 materials as-received and after recrystallization (denoted by -RC suffix), highlighting a large variation in the relative K concentration by 3−4 orders of magnitude among the 10 different samples. The relative SIMS intensities for other alkali cations, such as Li, Na, and Rb, only varied by ∼1 order of magnitude among the PbI_2 (Figure S5), which justifies our focus on K in relation to changes in device performance. As-received, AA5 displays K^+ intensity 2 orders of magnitude higher than TCI4, the second-highest quality and most pure reagent (see below). Hydrocarbon/carbohydrate (Figure 2a), oxide/hydroxide (Figure 2b), and nitrogen oxide (Figure 2c) SIMS fragment intensities suggest TCI4 and AA5 contain the lowest concentrations of oxygen-containing anion impurities (Figure 2a fragment intensities further reflect significant OAc impurity in SA2[28]). Together, these two measurements on AA5—low oxidic anion concentrations and I/Pb ratio greater than 2—imply that KI is the main impurity in this commercial source. For all reagents

https://doi.org/10.1021/acsaem.2c02842
ACS Appl. Energy Mater. 2023, 6, 295−301

except AA5, due to I/Pb ≤ 2, the K impurities can be regarded as KOH, KOAc, or KNO_3. Potassium iodide is known as a beneficial processing additive for perovskite devices,[20−25] and residual KI in AA5 plausibly explains the observation that AA5-derived perovskites always displayed the highest performing champion pixels across all three of our device data sets (Figures 1b and S1−S3). Finally, recrystallization reduced TOF-SIMS K^+ intensity in AA5 by nearly 3 orders of magnitude (Figure 1d). The relative decrease in other alkali cations was a maximum of ∼1 order of magnitude, again suggesting the large drop in K for AA5 is significant. Removing KI from a PbI_2 reagent free of anionic impurities is consistent with the observed decrease in the ICP-OES stoichiometry (Figure 1a) and lower device performance (Figure 1b) after recrystallization.

The stoichiometry and device results are only partially explained by OAc and KI impurities, suggesting perovskite material quality is sensitive to other trace impurities that are more difficult to identify. For example, increased nitrogen oxide SIMS intensities for AA4 (Figure 2c) suggest elevated nitrate impurities in this reagent that were removed by recrystallization (Figure S6). Indeed, several additional molecular impurities that might impact perovskite synthesis are visible by ^{1}H NMR of the as-received PbI_2s (Figure 3a). There are unassigned, hydrogen-containing impurities present in all as-received PbI_2 sources except AA5 (SA2 additionally showed a small impurity peak downfield at 10.7 ppm). Recrystallized materials in Figure 3b display reduced concentrations of original ^{1}H NMR impurities (comparing, e.g., the quartet at 3.54 ppm in AA4 and AA4-RC in Figure 3a,b, respectively) yet contain small signals from new impurities, one of which was identified as isopropanol (doublet at 0.99 ppm) that we used during filtration and collection. Additionally, integration of the H_2O peak before and after recrystallization reveals the H_2O in the PbI_2 are relatively low—1−2 orders of magnitude less than the original H_2O content of as-received, anhydrous dimethylsulfoxide (DMSO)-d_6 (∼0.02 M) despite being stored and only opened in a N_2 glovebox (see Table S3). This suggests negligible water was introduced from the recrystallization, likely due to the non-hygroscopic nature of PbI_2,[19] and the largest source of water in our perovskite processing may be unavoidable due to the hygroscopic *N*,*N*′-dimethlyformamide and DMSO solvents.

Overall, the NMR and additional SIMS data (Figures S5−S7) indicate the recrystallization decreases impurity concentrations in most categories, that is, the process indeed purifies the reagents. Successfully lowering impurity concentrations by recrystallization allowed us to observe a competition between detrimental and beneficial impacts of impurities, exemplified by the effects of OAc and K. Therefore, while recrystallizing PbI_2 may increase the purity, the degree to which the purified reagent improves the perovskite active layer and resulting devices may vary due to a given process's sensitivity to the trace beneficial impurities removed, as well as new trace species introduced, by the purification.

Consequently, researchers may leverage this information about the different major impurities in as-received PbI_2 reagents or incorporate a purification protocol to best suit their goals. Our observations help rationalize difficulties in reproducing results with PbI_2 from different suppliers or even batch-to-batch reproducibility from a single supplier. Improvements to purification methods and analytical characterization are necessary efforts for fundamental halide perovskite studies; an accurate quantification of the impact of impurities and additives requires first reducing their levels to negligible concentrations before titrating back into the reagents to isolate their effects. Ultimately, aqueous recrystallization methods may not achieve a desirable purity level nor optimal perovskite quality in devices, but alternative methods such as dissolution and precipitation from DMSO[11] or sublimation in the dark (to avoid photolysis[26,29,30]) under vacuum remain viable and could be simultaneously explored. Although the ideal purification technique relevant to perovskite semiconductors remains to be identified, fundamental and device-oriented research will benefit from deeper analytical insights into perovskite precursors and the resulting materials.

CONCLUSIONS

In summary, we studied a set of five commercial PbI_2 precursor sources often used to fabricate halide perovskite devices. Cumulative information gathered from three analytical chemistry techniques elucidate relationships between synthesis, I/Pb stoichiometry, impurities, properties, and performance. We substantiated our conclusions by performing purifications *via* aqueous recrystallization and evaluated its effectiveness. Our semiquantitative compositional analysis provides significant insights into specific impurities such as acetate and K that influence the functional performance of the resulting halide perovskite material. Identifying the remaining impurities and optimizing purification methods will help to clarify subtle yet impactful compositional variations that influence lab-to-lab or process-specific differences and contribute to perovskites reaching their full potential. Like all semiconductor materials preceding it, the halide perovskite technology will undoubtedly benefit from rigorous scrutiny of precursor composition and purification methods.

ASSOCIATED CONTENT

Supporting Information

The Supporting Information is available free of charge at https://pubs.acs.org/doi/10.1021/acsaem.2c02842.

Detailed materials lists, device fabrication, testing, and characterization methods, device *J*−*V* parameter statistics, performance results of two additional device composition architectures using the commercial PbI_2 reagents, ^{1}H NMR quantification of acetate figure, TOF-SIMS data, and tabulated H_2O quantification from ^{1}H NMR (PDF)

AUTHOR INFORMATION

Corresponding Author

David T. Moore − *National Renewable Energy Laboratory, Golden, Colorado 80401, United States;* orcid.org/0000-0003-3538-7586; Email: David.Moore@nrel.gov

Authors

Ross A. Kerner − *National Renewable Energy Laboratory, Golden, Colorado 80401, United States;* orcid.org/0000-0002-3692-6820

Earl D. Christensen − *National Renewable Energy Laboratory, Golden, Colorado 80401, United States;* orcid.org/0000-0001-7842-9294

Steven P. Harvey − *National Renewable Energy Laboratory, Golden, Colorado 80401, United States;* orcid.org/0000-0001-6120-7062

https://doi.org/10.1021/acsaem.2c02842
ACS Appl. Energy Mater. 2023, 6, 295−301

Jonah Messinger − *Department of Physics, University of Illinois Urbana-Champaign, Urbana, Illinois 61801, United States*

Severin N. Habisreutinger − *National Renewable Energy Laboratory, Golden, Colorado 80401, United States;* orcid.org/0000-0001-5760-8744

Fei Zhang − *National Renewable Energy Laboratory, Golden, Colorado 80401, United States; School of Chemical Engineering and Technology, Tianjin University, Tianjin 300072, China*

Giles E. Eperon − *Swift Solar Incorporated, San Carlos, California 94070, United States*

Laura T. Schelhas − *National Renewable Energy Laboratory, Golden, Colorado 80401, United States;* orcid.org/0000-0003-2299-1864

Kai Zhu − *National Renewable Energy Laboratory, Golden, Colorado 80401, United States;* orcid.org/0000-0003-0908-3909

Joseph J. Berry − *National Renewable Energy Laboratory, Golden, Colorado 80401, United States; Renewable and Sustainable Energy Institute and Department of Physics, University of Colorado Boulder, Boulder, Colorado 80309, United States;* orcid.org/0000-0003-3874-3582

Complete contact information is available at: https://pubs.acs.org/10.1021/acsaem.2c02842

Notes

The authors declare no competing financial interest.

■ ACKNOWLEDGMENTS

This work was authored by the National Renewable Energy Laboratory, operated by Alliance for Sustainable Energy, LLC, for the U.S. Department of Energy (DOE) under contract no. DE-AC36-08GO28308. Funding provided by the U.S. Department of Energy Office of Energy Efficiency and Renewable Energy, Solar Energy Technologies Office (SETO) project "De-risking Halide Perovskite Solar Cells" program (DE-FOA-0000990). R.A.K. acknowledges support from the Laboratory Directed Research and Development (LDRD) Program at NREL. The views expressed in the article do not necessarily represent the views of the DOE or the U.S. Government. The U.S. Government retains and the publisher, by accepting the article for publication, acknowledges that the U.S. Government retains a nonexclusive, paid-up, irrevocable, and worldwide license to publish or reproduce the published form of this work, or allow others to do so, for U.S. Government purposes.

■ REFERENCES

(1) Steirer, K. X.; Schulz, P.; Teeter, G.; Stevanovic, V.; Yang, M.; Zhu, K.; Berry, J. J. Defect Tolerance in Methylammonium Lead Triiodide Perovskite. *ACS Energy Lett.* **2016**, *1*, 360−366.

(2) Walsh, A.; Scanlon, D. O.; Chen, S.; Gong, X. G.; Wei, S.-H. Self-Regulation Mechanism for Charged Point Defects in Hybrid Halide Perovskites. *Angew. Chem., Int. Ed.* **2015**, *54*, 1791−1794.

(3) Yin, W.-J.; Shi, T.; Yan, Y. Unusual Defect Physics in $CH_3NH_3PbI_3$ Perovskite Solar Cell Absorber. *Appl. Phys. Lett.* **2014**, *104*, 063903.

(4) Zhang, X.; Turiansky, M. E.; Shen, J.-X.; Van de Walle, C. G. Iodine Interstitials as a Cause of Nonradiative Recombination in Hybrid Perovskites. *Phys. Rev. B* **2020**, *101*, 140101.

(5) Shin, D.; Zu, F.; Cohen, A. V.; Yi, Y.; Kronik, L.; Koch, N. Mechanism and Timescales of Reversible p-Doping of Methylammonium Lead Triiodide by Oxygen. *Adv. Mater.* **2021**, *33*, 2100211.

(6) Aristidou, N.; Eames, C.; Sanchez-Molina, I.; Bu, X.; Kosco, J.; Islam, M. S.; Haque, S. A. Fast Oxygen Diffusion and Iodide Defects Mediate Oxygen-Induced Degradation of Perovskite Solar Cells. *Nat. Commun.* **2017**, *8*, 15218.

(7) Bryant, D.; Aristidou, N.; Pont, S.; Sanchez-Molina, I.; Chotchunangatchaval, T.; Wheeler, S.; Durrant, J. R.; Haque, S. A. Light and Oxygen Induced Degradation Limits the Operational Stability of Methylammonium Lead Triiodide Perovskite Solar Cells. *Energy Environ. Sci.* **2016**, *9*, 1655−1660.

(8) Schoonman, J. The Ionic Conductivity of Pure and Doped Lead Bromide Single Crystals. *J. Solid State Chem.* **1972**, *4*, 466−474.

(9) Yao, J.; Yang, L.; Cai, F.; Yan, Y.; Gurney, R. S.; Liu, D.; Wang, T. The Impacts of PbI_2 Purity on the Morphology and Device Performance of One-step Spray-coated Planar Heterojunction Perovskite Solar Cells. *Sustainable Energy Fuels* **2018**, *2*, 436−443.

(10) Chang, J.; Zhu, H.; Li, B.; Isikgor, F. H.; Hao, Y.; Xu, Q.; Ouyang, J. Boosting the Performance of Planar Heterojunction Perovskite Solar Cell by Controlling the Precursor Purity of Perovskite Materials. *J. Mater. Chem. A* **2016**, *4*, 887−893.

(11) Senevirathna, D. C.; Yu, J. C.; Nirmal Peiris, T. A. N.; Li, B.; Michalska, M.; Li, H.; Jasieniak, J. J. Impact of Anion Impurities in Commercial PbI_2 on Lead Halide Perovskite Films and Solar Cells. *ACS Mater. Lett.* **2021**, *3*, 351−355.

(12) Chen, B.; Fei, C.; Chen, S.; Gu, H.; Xiao, X.; Huang, J. Recycling Lead and Transparent Conductors from Perovskite Solar Modules. *Nat. Commun.* **2021**, *12*, 5859.

(13) Lee, C.-H.; Shin, Y.-J.; Jeon, G. G.; Kang, D.; Jung, J.; Jeon, B.; Park, J.; Kim, J.; Yoon, S. J. Cost-*efficient*, Effect of Low-Quality PbI_2 Purification to Enhance Performances of Perovskite Quantum Dots and Perovskite Solar Cells. *Energies* **2021**, *14*, 201.

(14) Lee, C.-H.; Shin, Y.-J.; Villanueva-Antolí, A.; Das Adhikari, S. D.; Rodriguez-Pereira, J.; Macak, J. M.; Mesa, C. A.; Giménez, S.; Yoon, S. J.; Gualdrón-Reyes, A. F.; Mora-Seró, I. Efficient and Stable Blue- and Red-Emitting Perovskite Nanocrystals through Defect Engineering: PbX_2 Purification. *Chem. Mater.* **2021**, *33*, 8745−8757.

(15) Tsevas, K.; Smith, J. A.; Kumar, V.; Rodenburg, C.; Fakis, M.; Mohd Yusoff, A. R. b. M.; Vasilopoulou, M.; Lidzey, D. G.; Nazeeruddin, M. K.; Dunbar, A. D. F. Controlling PbI_2 Stoichiometry during Synthesis to Improve the Performance of Perovskite Photovoltaics. *Chem. Mater.* **2021**, *33*, 554−566.

(16) Min, H.; Kim, M.; Lee, S.-U.; Kim, H.; Kim, K.; Choi, J. H.; Lee, S. I.; Seok, S. I. Efficient, Stable Solar Cells by Using Inherent Bandgap of α-phase Formamidinium Lead Iodide. *Science* **2019**, *366*, 749−753.

(17) Zhang, Y.; Seo, S.; Lim, S. Y.; Kim, Y.; Kim, S.-G.; Lee, D.-K.; Lee, S.-H.; Shin, H.; Cheong, H.; Park, N.-G. Achieving Reproducible and High-Efficiency (>21%) Perovskite Solar Cells with a Presynthesized $FAPbI_3$ Powder. *ACS Energy Lett.* **2020**, *5*, 360−366.

(18) Tong, G.; Son, D.-Y.; Ono, L. K.; Kang, H.-B.; He, S.; Qiu, L.; Zhang, H.; Liu, Y.; Hieulle, J.; Qi, Y. Removal of Residual Compositions by Powder Engineering for High Efficiency Formamidinium-based Perovskite Solar Cells with Operation Lifetime Over 2000 h. *Nano Energy* **2021**, *87*, 106152.

(19) Tonn, J.; Matuchova, M.; Danilewsky, A. N.; Cröll, A. Removal of Oxidic Impurities for the Growth of High Purity Lead Iodide Single Crystals. *J. Cryst. Growth* **2015**, *416*, 82−89.

(20) Zhao, W.; Yao, Z.; Yu, F.; Yang, D.; Liu, S. Alkali Metal Doping for Improved $CH_3NH_3PbI_3$ Perovskite Solar Cells. *Adv. Sci.* **2018**, *5*, 1700131.

(21) Tang, Z.; Bessho, T.; Awai, F.; Kinoshita, T.; Maitani, M. M.; Jono, R.; Murakami, T. N.; Wang, H.; Kubo, T.; Uchida, S.; Segawa, H. Hysteresis-free Perovskite Solar Cells Made of Potassium-doped Organometal Halide Perovskite. *Sci. Rep.* **2017**, *7*, 12183.

(22) Abdi-Jalebi, M.; Andaji-Garmaroudi, Z.; Cacovich, S.; Stavrakas, C.; Philippe, B.; Richter, J. M.; Alsari, M.; Booker, E. P.; Hutter, E. M.; Pearson, A. J.; Lilliu, S.; Savenije, T. J.; Rensmo, H.; Divitini, G.; Ducati, C.; Friend, R. H.; Stranks, S. D. Maximizing and Stabilizing Luminescence from Halide Perovskites with Potassium Passivation. *Nature* **2018**, *555*, 497−501.

(23) Yang, Y.; Wu, L.; Hao, X.; Tang, Z.; Lai, H.; Zhang, J.; Wang, W.; Feng, L. Beneficial Effects of Potassium Iodide Incorporation on Grain Boundaries and Interfaces of Perovskite Solar Cells. *RSC Adv.* **2019**, *9*, 28561−28568.
(24) Son, D.-Y.; Kim, S.-G.; Seo, J.-Y.; Lee, S.-H.; Shin, H.; Lee, D.; Park, N.-G. Universal Approach toward Hysteresis-Free Perovskite Solar Cell via Defect Engineering. *J. Am. Chem. Soc.* **2018**, *140*, 1358−1364.
(25) Su, R.; Xu, Z.; Wu, J.; Luo, D.; Hu, Q.; Yang, W.; Yang, X.; Zhang, R.; Yu, H.; Russell, T. P.; Gong, Q.; Zhang, W.; Zhu, R. Dielectric Screening in Perovskite Photovoltaics. *Nat. Commun.* **2021**, *12*, 2479.
(26) Albrecht, M. G. The Photolysis of Lead Iodide. Ph.D. Thesis, University of London, Imperial College, 1975.
(27) Eckstein, J.; Erler, B.; Benz, K. W. High Purity Lead Iodide for Crystal Growth and Its Characterization. *Mater. Res. Bull.* **1992**, *27*, 537−544.
(28) NIST Standard Reference Database 69: NIST Chemistry WebBook Acetic acid (nist.gov). https://webbook.nist.gov/cgi/cbook.cgi?ID=C64197&Units=SI&Mask=200#Mass-Spec (accessed Nov 26, 2021).
(29) Saucedo, E.; Fornaro, L.; Mussio, L.; Gancharov, A. New Ways for Purifying Lead Iodide Appropriate as Spectrometric Grade Material. *IEEE Trans. Nucl. Sci.* **2002**, *49*, 1974−1977.
(30) Fornaro, L.; Saucedo, E.; Mussio, L.; Yerman, L.; Ma, X.; Burger, A. Lead Iodide Film Deposition and Characterization. *Nucl. Instrum. Methods* **2001**, *458*, 406−412.

https://doi.org/10.1021/acsaem.2c02842
ACS Appl. Energy Mater. 2023, 6, 295−301